

Modification of the Structure and Phase Composition of Structural Steel by a Microsecond E-Beam¹

Yu.F. Ivanov, Yu.A. Kolubaeva*, V.N. Devyatkov, O.V. Krygina*, N.N. Koval, P.V. Schanin

*Institute of High-Current Electronics, SB, RAS, 4 Akademichesky Ave., Tomsk, 634055, Russia,
(+3822)491713, (+3822)259410, yufi@opee.hcei.tsc.ru*

** Tomsk State University, Tomsk, Russia*

Abstract – The structure and phase composition of prehardened 38CrNi3MoVN steel subjected to an electron beam treatment have been studied by metallographic, scanning and transmission electron microscopy. The e-beam parameters are the following: the energy of accelerated electrons $U \approx 15$ keV, the beam current $I \approx 60$ A, the current pulse duration $\tau \approx 30$ μ s, the pulse repetition rate $f \approx 1$ Hz, the beam diameter in the specimen surface plane $D \approx 1.6$ cm, the beam energy density $E_S \approx 10$ J/cm². The e-beam treatment of the material has been shown to result in a gradient structure whose characteristic feature is a considerable (tens-fold) decrease in the average size of martensite crystallites and laths with attended increase in steel surface layer hardness by a factor of 2.5–3.

1. Introduction

At present one of the promising trends of physical materials science is modification of metal and alloy layers by intense energy flows (IEF's), among which are intense pulsed laser, electron and ion beams and plasma flows [1, 2]. When subjected to IEF's, the material is heated with extremely high rates, melted, and hardened that makes it possible to form amorphous nano- and submicrocrystalline structures in surface layers. Such noticeable changes in the structural-phase state of surface layers improve the physico-chemical and strength properties of the treated material that is unattainable with traditional methods of surface treatment [1–3].

The objective of the present work is to clarify the regularities of the evolution of the structural-phase state of structural steel surface layers treated by microsecond low-energy electron beam.

2. Materials and Experimental Procedure

The material to be tested was prehardened structural steel of composition Fe – 0.38 wt.% C – 1 wt.% Cr – 3 wt.% Ni – 0.8 wt.% Mo – 0.3 wt.% V. Electron-beam treatment was realized on the SOLO setup. The beam parameters were the following: the energy of accelerated electrons $U \approx 15$ keV, the beam current $I \approx 60$ A, the current pulse duration $\tau \approx 30$ μ s, the pulse

repetition rate $f \approx 1$ Hz, the beam diameter in the specimen surface plane $D \approx 1.6$ cm, the beam energy density $E_S \approx 10$ J/cm². The parameters of electron-beam treatment were: the number of pulses $N = 5, 10, 15, 20, 25, 30$, the pressure in the vacuum chamber $p \sim 10^{-2}$ Pa. The steel was examined by the methods of optical, scanning (SEM-515 “Philips”) and electron diffraction (TEM-125) microscopy. Mechanical tests of the material were performed by determining the microhardness at the irradiated surface, and the nanohardness of the specimen in depth (NHT-S-AX-000X, CSEM Instruments)

3. Results and Discussion

Pulsed electron-beam treatment led to melting of a steel layer of thickness ~ 25 – 30 μ m in the irradiation spot as evidenced by numerous microcraters and wavy relief of the preliminary polished specimen surface and by the dendritic structure of the steel in the spot that was clearly defined in metallographic examination of the etched section

High-rate melting and crystallization is accompanied by noticeable changes in the hardness of a steel layer of thickness ~ 110 – 120 μ m. However, the most drastic change of hardness was found in a surface layer hardened in the molten state (Fig. 1). It follows from analysis of the results presented in Fig. 1,a-c that this layer consists of several sublayers. The sublayer located at a depth of ~ 4 – 7 μ m displays the highest hardness. Increasing the number of pulses causes a decrease in hardness (from 1220 to 1050 kg/mm²), an increase in thickness (from 2 to 5 μ m) and in the occurrence depth (from 5 to 7 μ m) of this sublayer. The second (less pronounced) maximum of the nanohardness (~ 860 kg/mm²) is found in a sublayer located near the “melt-solid” interface. The material volume between the given sublayers also exhibits an increased (as compared to the initial state) hardness whose value is scarcely affected by the number of pulses. The smallest values of the nanohardness in the melt zone are observed near the irradiated surfaces. As the number of pulses is increased, the surface layer hardness increases (from 480 to 930 kg/mm²) and the minimum hardness “shifts” deep into the melt zone.

¹ The work was partially supported by the RF Ministry of Education and CRDF within the BRHE program “Physics and chemistry of high-energy systems” (project No. 016-02).

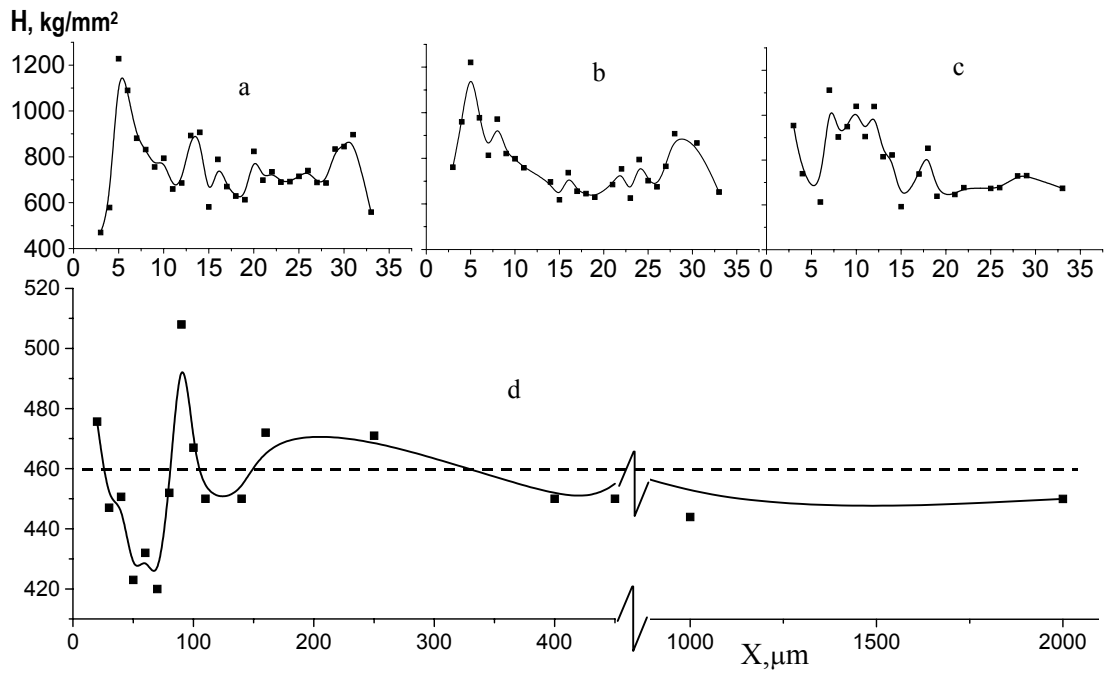


Fig. 1. Nanohardness (a–c) and microhardness (d) of the treated steel; a, d – $N = 10$, b – $N = 20$, c – $N = 30$ pulses. The microhardness of the steel before treatment $H_{\mu} \sim 460 \text{ kg/mm}^2$ (dotted line)

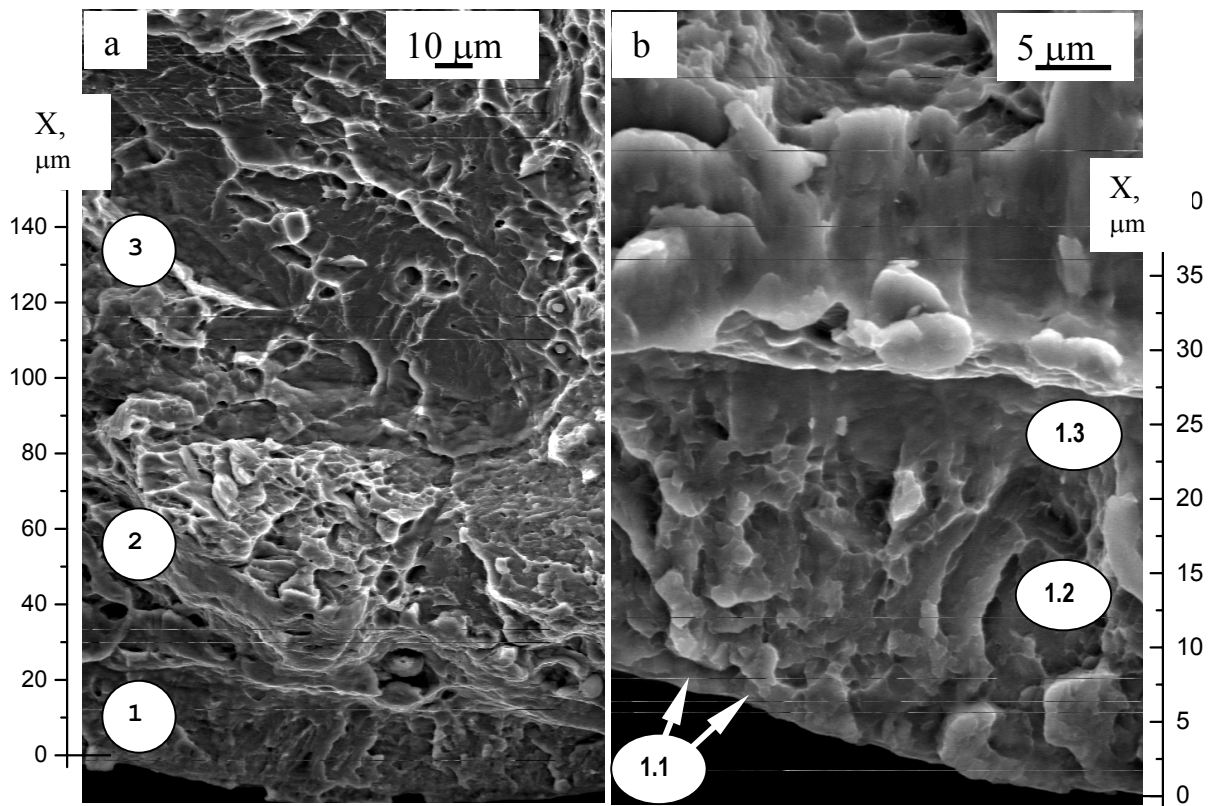


Fig. 2. Fracture surface of the steel treated by the electron beam. The layers are indicated as follows: 1 – near-surface, 2 – transition, 3 – main, 1.1 – surface, 1.2 – intermediate, 1.3 – transition. $N = 20$ pulses

The hardness of the layers resulted from solid-phase transformation of the steel that occurs under the action of heat liberated by the electron beam is lower than the hardness of the layer hardened in the molten state and is close to the values typical for the steel in the initial state (Fig. 1,d). Namely, the layer which is immediately adjacent to the melt zone and is located at a depth of $\sim 40\text{--}70\ \mu\text{m}$ displays a decreased hardness and the layer located at a depth of $\sim 90\text{--}100\ \mu\text{m}$ exhibits an increased value of this characteristic, as compared to the initial state.

The structural-phase transformations occurring in the steel under the action of the electron beam have been investigated by analyzing fractures (scanning electron microscopy) and thin foils (transmission electron microscopy). Characteristic images of the fracture surface of the irradiated steel are shown in Fig. 2. It can readily be seen that the electron-beam treatment results in a multilayer structure in a near-surface layer of the specimen volume. This structure consists of three extended layers: a near-surface layer (thickness $\sim 30\ \mu\text{m}$), a transition layer ($\sim 60\ \mu\text{m}$) and the main layer (Fig. 2,a). The near-surface layer has a characteristic columnar structure which indicates that this layer has resulted from crystallization of the melt. The transition layer is likely to be formed under the action of heat transferred to the specimen by the electron beam. The near-surface layer in turn consists of three clearly defined sublayers, namely: a surface sublayer (thickness $\sim 3\ \mu\text{m}$), an intermediate sublayer ($20\text{--}25\ \mu\text{m}$, and a transition sublayer ($5\text{--}8\ \mu\text{m}$) (Fig. 2,b). At the fracture surface of the intermediate sublayer there are clearly pronounced cleavage facets whose average size varies in the range $350\text{--}400\ \text{nm}$.

Comparison of the data presented in Figs. 1 and 2 allows us to point out the following. First, the maxi-

imum values of the nanohardness of the irradiated steel are achieved at the external and internal boundaries of the intermediate layer formed during crystallization of the melt. The value of the nanohardness of the intermediate layer volume therewith is comparatively low. Second, the minimum and maximum values of the microhardness are registered at the external and internal boundaries of the transition layer resulted from the solid-phase transformation of the steel under the action of heat of the electron beam. Third, the good agreement of the results obtained in analyzing the hardness profile and the structure of the fracture surface support the correctness of the procedure used to study the structure of the irradiated material.

The method of electron diffraction microscopy was employed to examine foils prepared from the material volume located at a depth of $\sim 200\ \mu\text{m}$. No considerable changes of the structure and phase state of the steel have been found. At a depth of $75\text{--}85\ \mu\text{m}$ (in the region of maximum microhardness), the martensite structure retains its initial morphology, effects of tempering of the steel with attendant precipitation of carbide phase particles and rearrangement of the dislocation substructure with the formation of fragments are clearly pronounced (Fig. 3). At a depth of $\sim 5\text{--}6\ \mu\text{m}$ (a material layer with a maximum nanohardness), a lath martensite structure dominates (Fig. 4).

A small number of nanocrystallites ($143 \pm 7\ \text{nm}$) of lenticular or equiaxial shapes appear only upon treatment with $N = 5$. The average size of laths and lath martensite crystals increases with increasing the number of pulses.

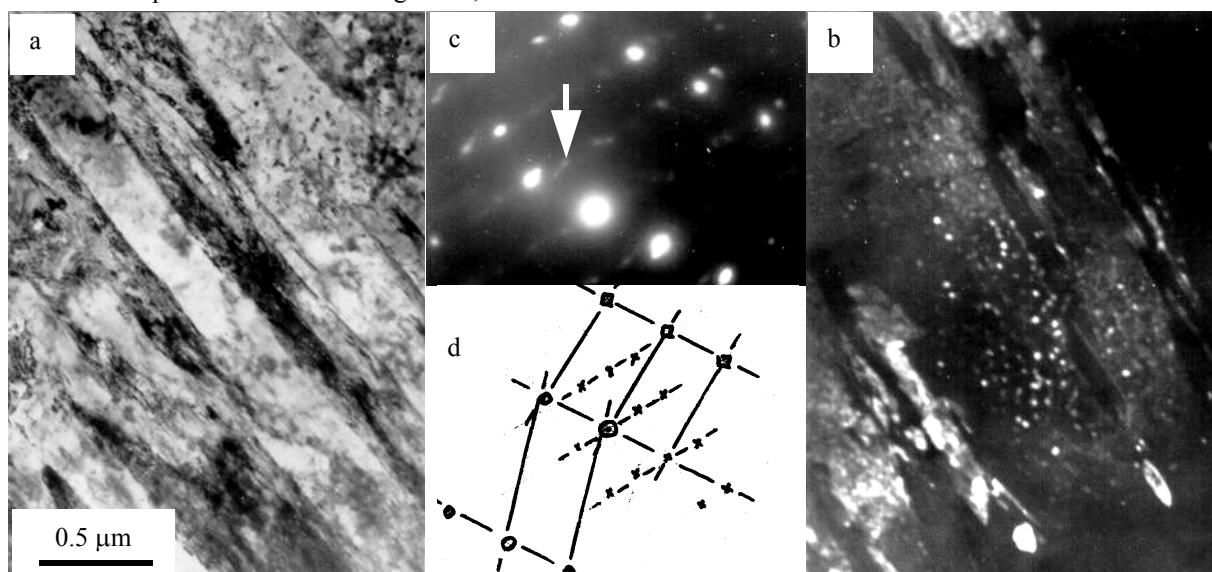


Fig. 3. TEM image of the 38CrNi3MoVN steel structure formed $75\ \mu\text{m}$ beneath the irradiated surface. $N = 30$ pulses. a – bright-field image; b – dark field in the reflex $[121]\text{Fe}_3\text{C}$; c – electron-diffraction pattern (the dark-field reflex is indicated by the arrow); d – indexing of the electron-diffraction pattern ($\Delta - (113)\alpha\text{-Fe}$; $x - (331)\alpha\text{-Fe}$; $o - (311)\text{Fe}_3\text{C}$)

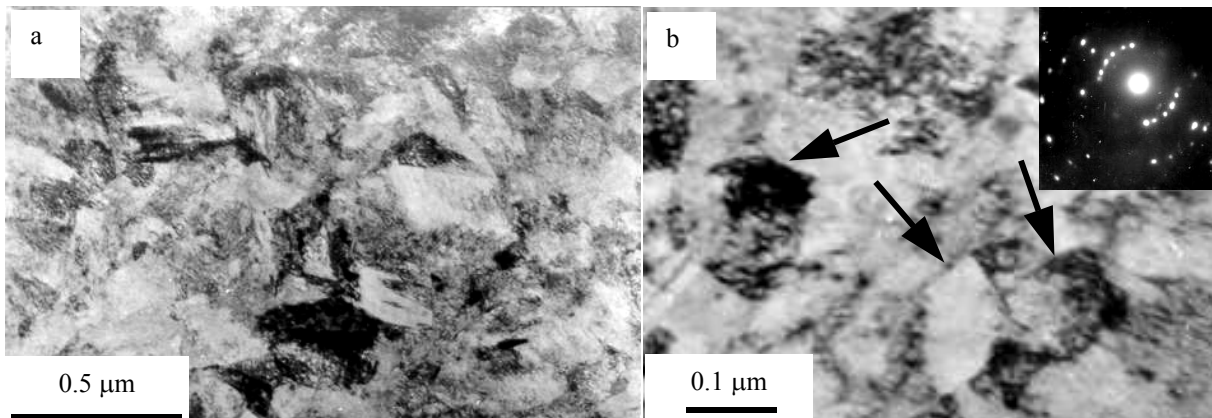


Fig. 4. TEM image of the 38CrNi3MoVN steel structure formed $\sim 3 \mu\text{m}$ beneath the irradiated surface. $N = 5$ pulses. Insert in (b) – electron-diffraction pattern taken from this part of the foil. Arrows on (b) stand for α -phase crystallites

The layer formed at the irradiated surface also has a martensite structure and can be related by its morphological features to lath martensite. A peculiarity of the structure of this layer is a considerably larger (5–10 times) size of the martensite structure elements (laths) and martensite crystals, as compared to the structure formed at a depth of $\sim 5\text{--}6 \mu\text{m}$. In the surface and near-surface layers hardened in the molten state the residual austenite is hardly detectable by electron diffraction microscopy.

4. Conclusion

Complex studies of the irradiated steel have revealed a multilayer structure of the material volume subjected to thermal e-beam treatment. It has been shown that the layers hardened in the molten state possess the

maximum hardness. One of the causes for the considerable (about threefold) increase in steel hardness is the formation of a martensite nanostructure in a near-surface layer.

References

- [1] *Modification and doping of surfaces by laser, ion, and electron beams*, Ed. By J. Poate, G. Foti and D (G) Jacobson, A.L. Peratt, Moscow, Mashinostroenie, 1987, 424 pp.
- [2] I.L. Pobel, *Thermal electron-beam treatment of metal materials*, *Itogi Nauki. i Tekh. Metalloved. i Term. Obr.*, Moscow, VINITI, 1990, pp. 99–166.
- [3] V.D. Sadovskii, V.M. Schastlivtsev, T.Ya. Tabatchikova, I.L. Yakovleva, *Laser heating and steel structure*, Sverdlovsk, UB, USSR AS, 1989, p. 101.